GSA Data Repository 2017101

Supplementary Information and Data Repository

Isotopic signature of dissolved iron delivered to the Southern Ocean from hydrothermal vents in the East Scotia Sea

Jessica K. Klar[1*], Rachael H. James[1], Dakota Gibbs[2,3], Alastair Lough[1], Ian Parkinson[4], J. Andrew Milton[1], Jeffrey A. Hawkes[5], and Douglas Connelly[2]

[1]*Ocean and Earth Science, University of Southampton Waterfront Campus, National Oceanography Centre Southampton, European Way, Southampton, SO14 3ZH, UK*

[2]*Marine Geosciences, National Oceanography Centre Southampton, European Way, Southampton, SO14 3ZH, UK*

[3]*Southern Cross Geoscience, Military Road, Lismore, NSW 2480, Australia*

[4]*School of Earth Sciences, University of Bristol, Queens Road, Bristol, BS8 1RJ, UK*

[5]*Department of Chemistry, Uppsala University, SE-751 05 Uppsala, Sweden*

*Current address: LEGOS (Laboratoire d'Etudes en Géophysique et Océanographie Spaciales), University of Toulouse, IRD, CNES, CNRS, UPS, 18 avenue Edouard Belin, 31401 Toulouse, France; E-mail: Jessica.klar@legos.obs-mip.fr

STUDY AREA

The ESR is a back-arc spreading center located in the East Scotia Sea in the Atlantic sector of the Southern Ocean (Fig. DR1). It is ~500 km long and consists of ten second-order ridge segments, from E1 in the north to E10 in the south, separated by non-transform faults. Hydrothermal activity has been detected on segments E2 and E9 (German et al., 2000; Rogers et al., 2012).

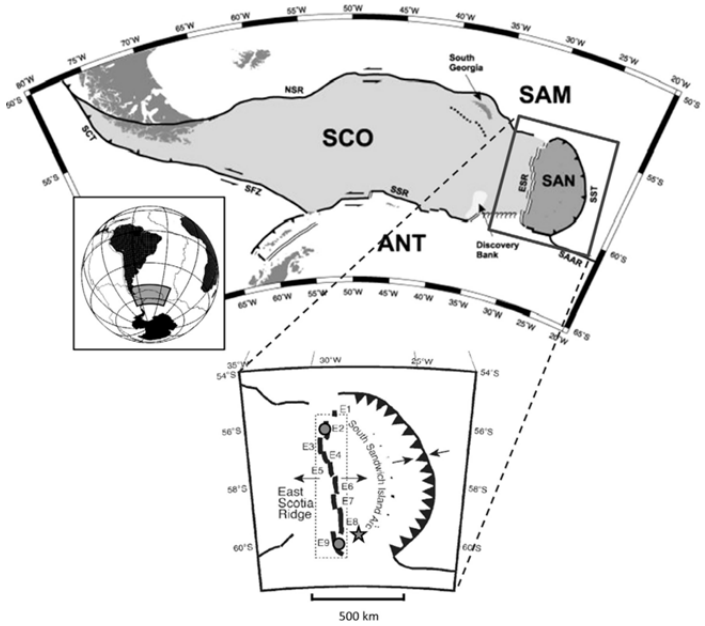

Figure DR1. Location of the study area, showing the East Scotia Ridge (ESR) and the South Sandwich Island Arc. ESR segments E1 to E9 are labelled and vent fields at E2 and E9 are indicated by the grey circles. SAM: South American plate; ANT: Antarctic plate; SCO: Scotia plate; SAN: Sandwich plate; SFZ: Shackleton Fracture Zone; NSR:

North Scotia Ridge; SSR: South Scotia Ridge; SCT: Southern Chile Trench; SST: South Sandwich Trench and SAAR: South American-Antarctic Ridge. Image from Cole et al. (2014).

Hydrothermal vent fluids from segment E2 have temperatures of up to 353 ºC (James et al., 2014) and low pH (~3.02), and endmember (zero Mg) concentrations of Fe and Mn range from, respectively, 790 to 1280 μM and from 2050 to 2220 μM. The chloride concentration of the endmember fluids (530 – 540 mM) is close to local bottom seawater (540 mM) and H_2S concentrations range from 6.7 to 7.1 mM (James et al., 2014). By contrast, vent fluids from the northernmost part of segment E9 (E9N) are hotter (up to 383 ºC) and the chloride concentration of the endmember fluid (98.2 mM) is distinctly lower than local bottom seawater, which is attributed to phase separation of the fluids (James et al., 2014). The pH of the vent fluids is between 3.08 and 3.42, and H_2S concentrations range from 9.5 to 14 mM. Concentrations of dFe in the endmember fluids (800 - 1210 μM) are similar to those measured at E2, whereas concentrations of dissolved Mn (~200 μM) are lower.

MATERIALS AND METHODS

Sample collection

Hydrothermal plumes were sampled on RRS *James Cook* cruises JC42 (2010, sampling of E2) and JC55 (2011, sampling of E9N). Hydrothermal plumes were detected and sampled using a SeaBird +911 CTD on a titanium (Ti) frame, equipped with up to 24 OTE (Ocean Testing Equipment) water sampling bottles, modified for trace metal

sampling (fitted with external springs and Teflon taps; and metallic components replaced with Ti). A light scattering sensor (LSS) and a bespoke redox potential (Eh) detector were also mounted onto the frame. The buoyant part of the hydrothermal plume was identified by positive temperature and particle (LSS) anomalies and a negative Eh anomaly, and was located at ~2580 m water depth at E2 and ~2380 m water depth at E9N. The neutrally buoyant plume was identified by a positive particle anomaly and negative temperature and Eh anomalies at 250 – 300 m above the sea floor (~2300 m water depth at E2 and ~2150 m water depth at E9N) (Fig. DR2).

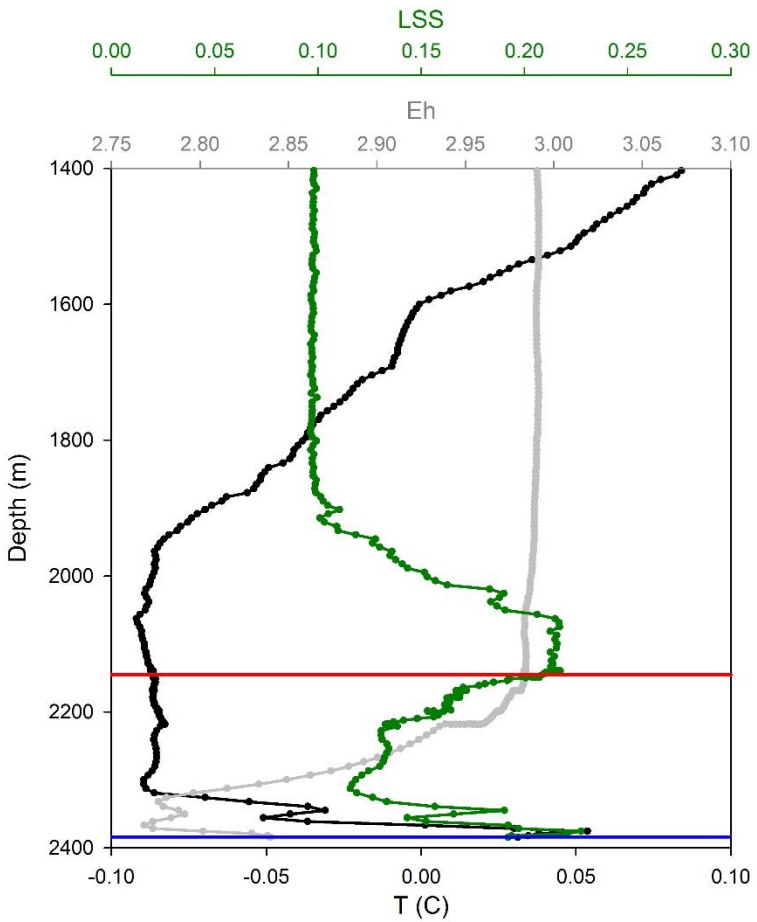

Figure DR2. Representative temperature (T), LSS and Eh profiles for the lowermost part of the water column at E9N. Blue line indicates depth of samples collected from the buoyant plume and red line indicates the depth of samples collected from the neutrally buoyant plume. For profiles corresponding to E2 plumes see Hawkes et al., (2013).

Upon recovery of the CTD, the OTE bottles were transferred to the clean lab container on board and seawater samples were filtered through a polycarbonate membrane filter (0.2 μm, Whatman) under gentle pressure using filtered oxygen-free nitrogen gas and collected in 500 ml acid-cleaned LDPE bottles. After filtration of ~ 10 L of seawater, the filters were kept for particulate metals concentration analysis. All seawater samples were then acidified to approximately pH 1.9 with thermally distilled nitric acid (Optima, Fisher Scientific). Sample bottles were bagged and shipped back to the laboratory for isotopic analysis.

Vent fluids were sampled during cruise JC42 using titanium (Ti) syringe samplers mounted on the Remotely Operated Vehicle (ROV) Isis. These Ti syringe samplers were equipped with an inductively coupled link (ICL) temperature sensor at the nozzle tip. Once the ROV was recovered on board, the fluids were transferred into 1 L acid cleaned HDPE bottles. The samplers were acidified to pH < 2 using thermally distilled nitric acid and shipped back to the laboratory for analysis.

Sampling Artifacts

It is important to note that the partitioning of Fe between Fe(II) and Fe(III) and different size fractions within the samples does not necessarily correspond to the partitioning of Fe within the plume at the time of sampling, as oxidation of dFe may occur between the time of tripping the sampling bottles and filtration (Bennett et al., 2009). The average time interval between sampling the hydrothermal plumes and sample filtration on deck was > 5 hours, which corresponds to > 3 Fe(II) half-lives in surrounding waters, or < 0.6 Fe(II) half-lives in the more acidic buoyant plume

(see 'Calculations of Fe(II) half-lives' below). This implies that there is high likelihood for continued oxidation of aqueous Fe(II) to Fe(III) and precipitation of Fe(III)-oxides within the OTE bottles during recovery. However, it is likely that oxidation rates in the OTE bottles are lower than calculated, as the bottles represent a closed rather than an open system. Although the buoyant plume samples contain a higher proportion of aqueous Fe(II) (see main text), they are also characterized by the slowest oxidation rates. As Fe sulfide precipitation and Fe(II) oxidation/Fe(III) precipitation occur in the early stages of vent fluid mixing with seawater, significant changes in redox speciation and size distribution of Fe, and therefore δ^{56}Fe, are unlikely, but cannot be ruled out.

Iron concentration and isotope analyses

All acids used for chemical processing of the samples were thermally distilled and regularly monitored for metal content. Milli-Q water was used for diluting acids and for cleaning. Low-density polyethylene (LDPE) sample bottles were cleaned for trace metal purposes using a three step cleaning procedure (2-3 days in 2.5 % Decon, 1 week in 50 % HCl and 1 week in 50 % HNO_3). The Teflon filtration unit (Savillex) used during the analytical procedure was cleaned in a similar manner, but the time in the acid baths was increased by a factor of 2. The unit was soaked in a 20 % HCl bath for at least a few hours between uses.

The concentration of dissolved metals (Fe and Mn) was determined by preconcentrating 100 ml of sample by mixed ligand extraction (Bruland et al., 1979), and analysis by inductively coupled plasma mass spectrometry (ICP-MS, Thermo Scientific X-Series). These results are reported in Hawkes et al. (2013). Fe concentrations were used to

inform optimum isotope spiking. The concentration of Fe in the particulate size fraction was determined by ICP-MS, after digesting the polycarbonate filters for 3 days at 150 °C in sub-boiled concentrated nitric acid, followed by drying down and redissolution in 3 % sub-boiled nitric acid (Hawkes et al., 2013).

Iron isotopes in the dissolved fraction (0.2 μm filtered) of hydrothermal plume samples were analyzed at the NOC following a similar procedure to that reported in John and Adkins (2010). Briefly, a sub-sample (100 to 500 ml) was taken into an acid cleaned LDPE bottle, and Fe was preconcentrated from the seawater using a NTA resin batch method. The Fe fraction was then purified by anion exchange chromatography (AG1-X8 resin). The procedure blank, specific for these samples, was 2.5 ± 0.5 ng Fe (n = 6). Aliquots of vent fluid samples were oxidized by treatment with concentrated nitric acid and hydrogen peroxide before purification by anion exchange using AG-MP1 resin following Homoky et al., (2013). The procedure blank was 0.69 ± 0.05 ng Fe (n=2).

Isotopic measurements were carried out in duplicate on a multi-collector inductively coupled plasma mass spectrometer (MC-ICP-MS) (Thermo Scientific Neptune) at the NOC. Instrumental mass bias was corrected using a ^{57}Fe-^{58}Fe double spike, which was added to the samples before chemical processing. ^{56}Fe/^{54}Fe ratios are expressed as δ^{56}Fe relative to the average ^{56}Fe/^{54}Fe value for the iron isotope reference material IRMM-014 determined during the analytical session ($\delta^{56}Fe = [(^{56}Fe/^{54}Fe)_{sample}/(^{56}Fe/^{54}Fe)_{IRMM\text{-}14} - 1] \times 1000$). The external precision and accuracy were assessed by multiple analyses of two iron isotope standards. The average δ^{56}Fe of the ETH (Eidgenössische Technische Hochschule Zürich) standard was 0.52 ± 0.06 ‰ (2SD, n=191) and the average in-house HEM standard was 0.25 ±

0.06 ‰ (2SD, n=174). The ETH standard is within analytical uncertainty of the consensus value of 0.52 ± 0.08 ‰ (2SD, n=80; Lacan et al., 2010). The analytical Fe separation method was validated by taking ETH standard through the AG-MP1 purification procedure, which yielded a δ^{56}Fe of 0.55 ± 0.05 ‰ (n=2).

Additional analyses

Salinity (conductivity), temperature and depth (pressure) were measured for each water column profile using a Seabird CTD sensor mounted on the rosette frame. Discrete samples of seawater for salinity analysis were taken from selected OTE bottles on cruise JC055 to cross-calibrate the sensors and to identify misfired bottles. This was not done on JC042. The CTD was also equipped with calibrated light scattering (LSS), Eh and oxygen sensors.

CALCULATIONS AND ISOTOPE MODELLING

Calculation of vent fluid and buoyant plume dilution factors

The extent of dilution of the vent fluid by seawater (VF dilution factor; x-axis in Figure 1 in the main text) is calculated from the Mn concentration of the plume sample: $VF\ dilution\ factor = ([Mn]_{VF} - [Mn]_{SW})/([Mn]_{sample} - [Mn]_{SW})$, where *[Mn]* represents the Mn concentration, *VF* represents the end member vent fluid, *SW* represents background seawater and *sample* represents the plume sample. $[Mn]_{VF} \approx 2050$ µM for E2 and $[Mn]_{VF} \approx 200$ µM for E9; $[Mn]_{SW} = 0.6$ nM (Table DR3). This calculation assumes that Mn behaves conservatively during mixing, due to its low reactivity and slow oxidation rate (Rudnicki and Elderfield, 1993).

Similarly, the extent of dilution of the buoyant plume (BP dilution factor; x-axis in Figure 3 of the main text) by surrounding seawater is calculated as: *BP dilution factor* = $([Mn]_{BP} - [Mn]_{SW})/([Mn]_{sample} - [Mn]_{SW})$, where *BP* represents the least dilute buoyant plume sample. $[Mn]_{BP} \approx 525$ nM for E2 and $[Mn]_{BP} \approx 34$ nM for E9N.

Calculation of Fe(II) half-lives

The Fe(II) half-life ($t_{1/2}=\ln 2/k_1$) in deep water masses surrounding E2 and E9 was calculated using the equations given in Millero et al., (1987):

$$k_1 = k[O_2][OH^-]^2 \qquad \text{Eq. 1}$$

$$\log k = 21.56 - 1545/T - 3.29I0.5 + 1.52I \qquad \text{Eq. 2}$$

$$I=19.9201S/(10^3-1.00488S) \qquad \text{Eq. 3}$$

Where k_1 is the pseudo first-order rate constant, k is the overall rate constant, $[O_2]$ is oxygen concentration in µmol/kg, $[OH^-]$ is hydroxide concentration in µmol/kg, T is temperature in degrees Kelvin, I is ionic strength and S is salinity. $[OH^-]$ was calculated from DIC and alkalinity measurements made on water samples collected during JC42 and JC55 (Hawkes et al., 2013), using the CO2Sys_v2.1 program (http://cdiac.ornl.gov/oceans/co2rprt.html). ESS deep water T, S and O_2 were obtained from WOA (https://www.nodc.noaa.gov/OC5/woa13/) stations 5481(B) and 3978(B). The Fe(II) half-life in waters surrounding E2 and E9 is 1.49 ± 0.10 hours (n = 16). The Fe(II) half-life is considerably longer (up to 8.5 h) in the slightly more acidic buoyant plumes at both sites.

Modelling of the isotopic fractionation during Fe(II) oxidation in the buoyant plume

Iron delivered by hydrothermal vents is initially in the reduced aqueous Fe(II) form (e.g., Statham et al., 2005). Immediately on venting at the seafloor, some of this iron precipitates as iron sulfides (e.g., Rudnicki and Elderfield, 1993) which leads to enrichment in heavier Fe isotopes of the remaining dFe, as described in the main text. Thus vent fluids that originally have δ^{56}Fe = -0.28 ‰ (E2) and δ^{56}Fe = -0.30 ‰ (E9N) have, respectively δ^{56}Fe values of +0.07 ± 0.05 ‰ (E2) and +0.49 ± 0.05 ‰ (E9N) after sulfide precipitation (see main text for details).

As the vent fluids mix with oxic seawater, Fe(II) starts to oxidize to aqueous Fe(III), which rapidly precipitates as Fe(III)-oxides. The Fe(III) preferentially incorporates heavier isotopes, leaving the remaining Fe(II) up to 3.56 ‰ lighter (Welch et al., 2003). The effect of Fe(II) oxidation on δ^{56}Fe can be modelled in terms of Raleigh distillation, where Fe(II) is always in the dissolved phase and Fe(III) precipitates from solution and is isolated from the aqueous Fe(II) species (i.e., equilibrium is not attained). The isotopic compositions of the remaining Fe(II) and the accumulated Fe(III) precipitate are therefore given by:

$$\delta^{56}Fe(II) = (\delta^{56}Fe(II)_0 + 1000) * f^{\propto -1} - 1000 \qquad \text{Eq. 4}$$

$$\delta^{56}Fe(III) = \frac{1-f^{\alpha}}{1-f}(\delta^{56}Fe(II)_0 + 1000) - 1000 \qquad \text{Eq. 5}$$

where $\delta^{56}Fe(II)$ is the isotopic ratio of the remaining Fe(II), $\delta^{56}Fe(II)_0$ is the initial isotopic ratio of Fe(II) before oxidation starts (corrected for sulfide precipitation), $\delta^{56}Fe(III)$ is the isotopic ratio of the accumulated precipitated

Fe(III) and α is the fractionation factor between aqueous Fe(II) and precipitated Fe(III), $\alpha_{Fe(III)\text{-}Fe(II)}$ at a temperature of -0.09 °C (α=1.0036; Welch et al., 2003).

The Fe(III)-oxide particles are most likely distributed across a wide spectrum of particle sizes, including the colloidal size fraction (0.02 – 0.2 μm). Therefore, the dissolved size fraction (< 0.2 μm) is initially entirely composed of Fe(II), but as Fe(II) oxidation starts, an increasing proportion of the dissolved fraction will also consist of colloidal Fe(III) particles. As the Fe(III) aggregates into larger particles and leaves the dissolved size fraction, the isotopic composition of Fe remaining in the dissolved fraction is altered. Hence δ^{56}Fe of dFe delivered to the buoyant plume is modelled as a function of the fraction (*f*) of Fe remaining as Fe(II) and the proportion (*X*) of Fe(III) that remains in the dissolved (colloidal) phase:

$$\delta^{56}Fe = \frac{f*\delta^{56}Fe(II)+X*(1-f)*\delta^{56}Fe(III)}{f+X*(1-f)} \qquad \text{Eq. 6}$$

This model assumes that a constant proportion of Fe(III) is lost from the dissolved phase throughout the oxidation process. In reality, the rate of Fe(III)-oxide particle coagulation will vary over time, with highest rates at lowest plume dilution, where highest Fe and particle concentrations are found.

DATA

Table DR1. Concentrations of Mg, Mn and Fe and Fe isotopic compositions in high-temperature hydrothermal vent fluids sampled at vent sites E2 and E9N.

	Mg (mM)	Mn (μM)	Fe (μM)	δ^{56}Fe (‰)	2 SD (‰)
E2	1.64	2020	1066	-0.28	0.05
E9N	0.59	200	578	-0.30	0.05

Table DR2. Sample locations, concentrations of dissolved and total (dissolved + particulate) Fe (tFe) and dissolved Mn (dMn), dFe isotopic composition and calculated vent fluid dilution factor in buoyant (grey shading) and neutrally buoyant plume samples.

Sample	Lat (°N)	Long (°E)	Depth (m)	VF Dilution factor	dMn (nM)	dFe (nM)	tFe (nM)	δ^{56}Fe (‰)	2 SD (‰)
E2, Cruise JC042									
3-01	-56.088	-30.319	2586	5900	348	36.1	144	-0.88	0.07
3-06	-56.088	-30.319	2574	3900	525	83.5	229	-1.19	0.11
3-07	-56.088	-30.319	2372	18000	112	20.2	N.D.	-0.75	0.06
3-11	-56.088	-30.319	2277	14000	147	30.9	50	-0.69	0.07
5-01	-56.089	-30.319	2567	5800	354	31.6	168	-1.10	0.07
7-02	-56.089	-30.318	2272	37000	56.4	12.1	18	-0.43	0.07
7-11	-56.089	-30.318	2272	21000	97.6	14.3	20	-0.66	0.10
7-13	-56.089	-30.318	2272	35000	58.3	18.0	24	-0.56	0.10
7-17	-56.089	-30.318	2272	28000	73.2	13.1	20	-0.29	0.07
E9N, Cruise JC055									
424-04	-60.043	-29.982	2382	7400	27.3	14.0	18	-0.23	0.09
424-07	-60.043	-29.982	2385	5800	34.8	23.0	27	-0.76	0.06
424-10	-60.043	-29.982	2144	35000	6.31	7.31	9	-0.29	0.05
424-14	-60.043	-29.982	2146	12000	10.6	10.9	17	-0.21	0.18

N.D: no data

Table DR3. Concentration of dMn measured outside of the hydrothermal plumes in the East Scotia Sea. Average value = 0.6 ± 0.3 nM.

Sample	Lat (°N)	Long (°E)	Depth (m)	dMn (nM)
JC42-03-14	-56.088	-30.319	1000	0.28
JC42-04-17	-56.089	-30.318	2349	0.81
JC42-04-23	-56.089	-30.318	995	0.18
JC42-08-17	-56.089	-30.315	1000	0.40
JC42-10-18	-60.043	-28.982	1498	0.41
JC55-422-01	-59.682	-33.103	2350	0.96
JC55-422-02	-59.682	-33.103	2350	0.93
JC55-422-03	-59.682	-33.103	2350	0.30
JC55-422-13	-59.682	-33.103	2000	0.98
JC55-422-14	-59.682	-33.103	2000	0.20
JC55-422-15	-59.682	-33.103	2000	0.40
JC55-424-08	-60.043	-29.982	2218	0.69
JC55-424-22	-60.043	-29.982	1750	0.87

REFERENCES CITED

Bruland, K. W., Franks, R. P., Knauer, G. A., and Martin, J. H., 1979, Sampling and analytical methods for the determination of copper, cadmium, zinc, and nickel at the nanogram per liter level in sea-water: Analytica Chimica Acta, v. 105, no. 1, p. 233-245, doi:10.1016/s0003-2670(01)83754-5.

Cole, C. S., James, R. H., Connelly, D. P., and Hathorne, E. C., 2014, Rare earth elements as indicators of hydrothermal processes within the East Scotia subduction zone system: Geochimica et Cosmochimica Acta, v. 140, no. 0, p. 20-38, doi:10.1016/j.gca.2014.05.018.

German, C. R., Livermore, R. A., Baker, E. T., Bruguier, N. I., Connelly, D. P., Cunningham, A. P., Morris, P., Rouse, I. P., Statham, P. J., and Tyler, P. A., 2000, Hydrothermal plumes above the East Scotia Ridge: an isolated high-latitude back-arc spreading centre: Earth and Planetary Science Letters, v. 184, no. 1, p. 241-250, doi:10.1016/s0012-821x(00)00319-8.

Hawkes, J. A., Connelly, D. P., Gledhill, M., and Achterberg, E. P., 2013, The stabilisation and transportation of dissolved iron from high temperature hydrothermal vent systems: Earth and Planetary Science Letters, v. 375, no. 0, p. 280-290, doi:10.1016/j.epsl.2013.05.047.

Homoky, W. B., John, S. G., Conway, T. M., and Mills, R. A., 2013, Distinct iron isotopic signatures and supply from marine sediment dissolution: Nat Commun, v. 4, doi:10.1038/ncomms3143.

James, R. H., Green, D. R. H., Stock, M. J., Alker, B. J., Banerjee, N. R., Cole, C., German, C. R., Huvenne, V. A. I., Powell, A. M., and Connelly, D. P., 2014, Composition of hydrothermal fluids and mineralogy of associated chimney material on the East Scotia Ridge back-arc spreading centre: Geochimica et Cosmochimica Acta, v. 139, no. 0, p. 47-71, doi:10.1016/j.gca.2014.04.024.

John, S. G., and Adkins, J. F., 2010, Analysis of dissolved iron isotopes in seawater: Marine Chemistry, v. 119, p. 65-79, doi:10.1016/j.marchem.2010.01.001.

Lacan, F., Radic, A., Labatut, M., Jeandel, C., Poitrasson, F., Sarthou, G., Pradoux, C., Chmeleff, J., and Freydier, R., 2010, High-Precision Determination of the Isotopic Composition of Dissolved Iron in Iron Depleted Seawater by Double Spike Multicollector-ICPMS: Analytical Chemistry, v. 82, no. 17, p. 7103-7111, doi:10.1021/ac1002504.

Millero, F. J., Sotolongo, S., and Izaguirre, M., 1987, The oxidation-kinetics of Fe(II) in seawater: Geochimica et Cosmochimica Acta, v. 51, no. 4, p. 793-801, doi:10.1016/0016-7037(87)90093-7.

Rogers, A. D., Tyler, P. A., Connelly, D. P., Copley, J. T., James, R., Larter, R. D., Linse, K., Mills, R. A., Garabato, A. N., Pancost, R. D., Pearce, D. A., Polunin, N. V. C., German, C. R., Shank, T., Boersch-Supan, P. H., Alker, B. J., Aquilina, A., Bennett, S. A., Clarke, A., Dinley, R. J. J., Graham, A. G. C., Green, D. R. H., Hawkes, J. A., Hepburn, L., Hilario, A., Huvenne, V. A. I., Marsh, L., Ramirez-Llodra, E., Reid, W. D. K., Roterman, C. N., Sweeting, C. J., Thatje, S., and Zwirglmaier, K., 2012, The Discovery of New Deep-Sea Hydrothermal Vent Communities in the Southern Ocean and Implications for Biogeography: Plos Biology, v. 10, no. 1, doi:10.1371/journal.pbio.1001234.

Rudnicki, M. D., and Elderfield, H., 1993, A chemical model of the buoyant and neutrally buoyant plume above the TAG vent field, 26 degrees N, Mid-Atlantic Ridge: Geochimica et Cosmochimica Acta, v. 57, no. 13, p. 2939-2957, doi:10.1016/0016-7037(93)90285-5.

Statham, P. J., German, C. R., and Connelly, D. P., 2005, Iron(II) distribution and oxidation kinetics in hydrothermal plumes at the Kairei and Edmond vent sites, Indian Ocean: Earth and Planetary Science Letters, v. 236, no. 3-4, p. 588-596, doi:10.1016/j.epsl.2005.03.008.

Welch, S. A., Beard, B. L., Johnson, C. M., and Braterman, P. S., 2003, Kinetic and equilibrium Fe isotope fractionation between aqueous Fe(II) and Fe(III): Geochimica et Cosmochimica Acta, v. 67, no. 22, p. 4231-4250, doi:10.1016/S0016-7037(03)00266-7.